Charge and spin-dependent thermal efficiency of polythiophene molecular junction in presence of dephasing

Z. Golsanamlou[†], M. Bagheri Tagani, and H. Rahimpour Soleimani[‡]

Department of Physics, University of Guilan, P. O. Box 41335-1914, *Rasht, Iran*

(Received 23 February 2015; revised manuscript received 6 May 2015; published online 20 August 2015)

The charge and spin-dependent thermoelectric properties of different lengths of polythiophene in a molecular junction are investigated using the Büttiker probe method within Green function formalism in linear response regime. The coupling of the molecular chain to three-dimensional ferromagnetic electrodes is described by a tight-binding model for both parallel and antiparallel spin configurations. The decrease of height of transmission probability peaks and thermoelectric coefficients are observed in the presence of the Büttiker probes. The reduction is more intensive in the strong dephased chains. Results show that the spin magnetothermopower is bigger than the charge magnetothermopower due to the larger difference between the spin thermopowers with respect to the charge ones. In addition, we observed that the kind of carriers participating in the thermoelectric transport depends on the number of the thiophene rings.

Keywords: polythiophene, Green function, thermoelectric coefficients, Büttiker probes, ferromagnetic electrodes

PACS: 84.60.Rb, 75.76.+j, 73.63.Rt **DOI:** 10.1088/1674-1056/24/10/108402

1. Introduction

The dephasing process in molecular systems is an interesting phenomena that has attracted the attention of researchers. Dephasing in real systems can be made of electron–phonon interaction, defects, impurities, etc., which destroy the phase of electrons in the transport mechanism.[1–5] A well-known way to take into account the dephasing process or inelastic scattering in nanosystems is to use additional Büttiker probes.[6] D'Amato and Pastawski studied the conductance in a disordered linear chain.[7] The chain length was considered to be finite and incoherent scattering processes on a tight-binding (TB) model were studied using Büttiker probe model.

Study of charge and spin-dependent thermoelectric properties has become a popular topic in recent years for conversion of induced thermal energy to electric energy.[8,9] The thermal efficiency depends on dimensionless quantity as a figure of merit, $ZT = S^2 G_e T/\kappa$ which is a function of thermopower (S), operating temperature (T), electrical and thermal conductances, G_e and κ. The efficiency of the thermoelectric nanodevices to convert a temperature gradient into spin voltage can be determined by spin figure of merit, $Z_s T = |S_s^2 G_s T/\kappa|$ where, T is the operating temperature. G_s and κ are spin and thermal conductances, respectively. S_s denotes spin thermopower that is obtained in absence of charge and spin currents.[10] Because of the probability of the negative value for G_s, the $Z_s T$ takes an absolute value. The molecular devices can have the ZT higher than unity denoting they can work as a good thermoelectric device.[11]

Because of the unique properties of π-conjugated polymers like HOMO-LUMO (highest occupied molecular orbital–lowest unoccupied molecular orbital) gap, spin–orbit coupling, high carrier mobility, low conductivity and easy synthesis,[8,12–14] they are mainly considered for thermoelectric studies.[15,16] One of the famous polymers is polythiophene (PT) with thiophene rings which are in antiposition structure. The stable state of this polymer and maximum conductance are occurred in a flat geometry of the thiophene rings because of the lower HOMO–LUMO gap than twisted one.[17] Also, the electrical conductivity of PT can be increased by n-doping and p-doping agents.[18] Therefore, PT has been selected as a good choice for molecular investigations.[19–21] The length dependent study of thermoelectric properties has been attracted considerable attention from researchers.[22,23]

Datta *et al.*[24] studied a simple phenomenological approach to regard dephasing process in quantum transport models using Green function formalism. They introduced two specific self-energies: one for momentum conservation and the other for momentum relaxation. They found that the first case affects phase relaxation length but the second one affects both phase and momentum relaxation lengths. The multi-terminal electron transport was studied through a single phenalenyl molecule[25] using TB model and Green function formalism. It was observed that the electron transport depends on molecule–electrodes interface geometry, the presence of other electrodes, and the strength of molecular coupling to the side connected electrodes.

In the present work, we study the effect of dephasing on the charge and spin thermoelectric properties of different

[†]Corresponding author. E-mail: zahra.golsanamlou@gmail.com
[‡]Corresponding author. E-mail: rahimpour@guilan.ac.ir

© 2015 Chinese Physical Society and IOP Publishing Ltd

lengths of PT molecule coupled to the three dimensional ferromagnetic (FM) electrodes using Green function formalism in linear response regime, which has not been reported so far. The outline of this paper is as follows: in Section 2, we describe our theoretical method using Su–Schrieffer–Heeger (SSH) model[26] for Hamiltonian of the PT molecule and TB model for electrode–PT coupling. We account for the dephasing effect in our calculation by Büttiker probe method and D'Amato calculations.[7] Our numerical results are presented in Section 3. Finally a brief conclusion is given at the end of the paper.

2. Model and formalism

We consider the Keldysh nonequilibrium Green function formalism to calculate, respectively, the charge, heat, and spin currents, in presence of dephasing, as follows:[27–29]

$$J_{\rm e} = \frac{e}{h}\sum_{\sigma}\int {\rm d}\varepsilon[f_L(\varepsilon)-f_R(\varepsilon)]T_{{\rm eff}\sigma}(\varepsilon), \tag{1a}$$

$$J_Q = \frac{1}{h}\sum_{\sigma}\int {\rm d}\varepsilon(\varepsilon-\mu_L)[f_L(\varepsilon)-f_R(\varepsilon)]T_{{\rm eff}\sigma}(\varepsilon), \tag{1b}$$

$$J_{\rm s} = \frac{1}{h}\sum_{\sigma}\int {\rm d}\varepsilon\frac{\hbar}{2}\sigma[f_L(\varepsilon)-f_R(\varepsilon)]T_{{\rm eff}\sigma}(\varepsilon), \tag{1c}$$

where, $f_{L(R)}(\varepsilon) = [1+\exp((\varepsilon-\mu_L)/kT_L)]^{-1}$ is the Fermi–Dirac distribution function of electrode $L(R)$, μ_L and T_L denote the chemical potential and temperature of the electrode L, respectively. $T_{{\rm eff}\sigma}$ is the spin-dependent effective transmission coefficient of the disordered system and the total effective transmission coefficient of the carriers is as follows:

$$T_{\rm eff}(\varepsilon) = \sum_{\sigma} T_{{\rm eff}\sigma}, \tag{2}$$

where, $T_{{\rm eff}\sigma}$ is calculated using the D′Amato–Pastawski model:[7]

$$T_{{\rm eff}\sigma}(\varepsilon) = T_{LR\sigma}(\varepsilon) + \sum_{k,m=1}^{N} T_{Rk\sigma}(\varepsilon)W^{-1}_{km\sigma}(\varepsilon)T_{mL\sigma}(\varepsilon), \tag{3}$$

here, the first term on the right-hand side of the above equation describes the coherent transport, whereas the second term describes the transport in the presence of the phase breaking process. $W_{km\sigma}$ is given as

$$W_{km\sigma} = \delta_{km}(1-R_{km\sigma}) - (1-\delta_{km})T_{km\sigma}, \tag{4}$$

where, the reflection probability, $R_{kk\sigma}$, and transmission probability, $T_{km\sigma}$ are:

$$R_{kk\sigma} = 1 - \sum_{k\neq m} T_{km\sigma}, \tag{5a}$$

$$T_{km\sigma} = {\rm Tr}[\Gamma_{k,\sigma}G^r_{\sigma}\Gamma_{m,\sigma}G^a_{\sigma}], \tag{5b}$$

where, $\Gamma_{k,\sigma}$ are the spin-dependent broadening functions of the fictitious electrodes and are the same for all atomic sites in the chain.

The retarded Green function of the PT molecule coupled to the FM electrodes (Fig. 1(a) in presence of dephasing is written as follows:

$$G^r_{\sigma}(\varepsilon, V_{\rm G}) = [(\varepsilon+{\rm i}0^+)I - H_{\rm m} - \Sigma_{L,\sigma}(\varepsilon) - \Sigma_{R,\sigma}(\varepsilon) - \Sigma_D]^{-1}, \tag{6}$$

where, 0^+ is an infinitesimal value. $H_{\rm m}$ denotes the Hamiltonian of the molecule via an extended SSH model:[30,31]

$$\begin{aligned} H_{\rm m} =& \sum_{i,\sigma}\left\{(\varepsilon_i + eV_{\rm G})c^{\dagger}_{i,\sigma}c_{i,\sigma} - t_{i,i+1}(c^{\dagger}_{i+1,\sigma}c_{i,\sigma} + {\rm h.c})\right\} \\ & - \sum_{i,\sigma}\left\{\varepsilon_{\rm s}(c^{\dagger}_{4i-3,\sigma}c_{4i-3,\sigma} + c^{\dagger}_{4i,\sigma}c_{4i,\sigma}) + t_{\rm s}(c^{\dagger}_{4i-3,\sigma}c_{4i,\sigma} + {\rm h.c.})\right\} \\ & + K_0/2\sum_i (u_{i+1}-u_i)^2. \end{aligned} \tag{7}$$

Here, ε_i is the on-site energy and $V_{\rm G}$ refers to the gate voltage used to tune the molecular energy levels. $c^{\dagger}_{i,\sigma}(c_{i,\sigma})$ creates (annihilates) a π-electron with spin σ at the lattice site i. The effect of a sulfur atom on the Hamiltonian of the PT molecule is described by $\varepsilon_{\rm s}$ and $t_{\rm s}$. Other input parameters of the above equation are: the elastic constant K_0 and the lattice displacement at site i, u_i.[32] The hopping parameter between i-th and $(i+1)$-th sites of the molecule is as follows:

$$t_{i,i+1} = t_0 - t_1\cos({\rm i}\pi/2) - \alpha(u_{i+1}-u_i), \tag{8}$$

where, t_1, t_0, and α are the non-degeneracy parameter, zero displacement hopping integral, and electron-lattice coupling constant, respectively.[33] To obtain u_i, the Schrödinger equation can be solved for the electronic part of the Hamiltonian to find the electronic eigenstates $|\psi_{\mu,\sigma}\rangle = \sum_j \chi_{j,\mu,\sigma}c^{\dagger}_{j,\sigma}|0\rangle$ and eigenvalues $\varepsilon_{\mu,\sigma}$, as follows:[30,31]

$$\begin{aligned} & \varepsilon_j\chi_{j,\mu,\sigma} - t_{j,j+1}\chi_{j+1,\mu,\sigma} - t_{j,j-1}\chi_{j-1,\mu,\sigma} \\ & \quad - (\varepsilon_{\rm s}\chi_{j,\mu,\sigma} + t_{\rm s}\chi_{j-3,\mu,\sigma})\Delta(j/4,{\rm int}) \\ & \quad - (\varepsilon_{\rm s}\chi_{j,\mu,\sigma} + t_{\rm s}\chi_{j+3,\mu,\sigma})\Delta(j-3/4,{\rm int}) \\ & = \varepsilon_{\mu,\sigma}\chi_{j,\mu,\sigma}, \end{aligned} \tag{9}$$

where,

$$\Delta(x,{\rm int}) = \begin{cases} 1, & x = {\rm integer}, \\ 0, & {\rm otherwise}. \end{cases} \tag{10}$$

The displacement of ith carbon atom can be determined by minimizing the total energy of the system;

$$\begin{aligned} u_j =& 1/2\Big[u_{j-1} + u_{j+1} \\ & + 2\alpha/K_0\sum_{\mu,\sigma}^{occ}\left(\chi_{j+1,\mu,\sigma}\chi_{j,\mu,\sigma} - \chi_{j,\mu,\sigma}\chi_{j-1,\mu,\sigma}\right)\Big], \end{aligned} \tag{11}$$

Equations (9) and (11) should be solved in a self-consistent manner. Our model describes the π-electron system of the PT connected to the semi-infinite FM electrodes with a simple cubic structure. The electrodes have a square cross section (x–y plane) because the electron transport happens through the

central point at the cross section connected to the end of the molecular chain, see Fig. 1(a). H_α indicates the Hamiltonian of the $\alpha\,(=L$ or $R)$ FM electrode, which is written as:

$$H_\alpha = \sum_{k_\alpha,\sigma} (\varepsilon_0 - \sigma.J_\alpha) d^\dagger_{k_\alpha,\sigma} d_{k_\alpha,\sigma} - t(d^\dagger_{k_\alpha,\sigma} d_{k_\alpha+1,\sigma} + d^\dagger_{k_\alpha+1,\sigma} d_{k_\alpha,\sigma}), \tag{12}$$

where, $d^\dagger_{k_\alpha,\sigma}\,(d_{k_\alpha,\sigma})$ is the creation (annihilation) operator of an electron with spin σ at site k in electrode α. ε_0 and t denote the on-site energy and the hopping matrix element in electrodes, respectively. J_α is the integral exchange energy and σ denotes the conventional Pauli spin operator. The coupling between the molecule and electrodes is given by:

$$H_T = \sum_i t_{\mathrm{c(i,\sigma,k)}} (d^\dagger_{k,\sigma} c_{i,\sigma} + \mathrm{h.c.}), \tag{13}$$

where, $t_{\mathrm{c(i,\sigma,k)}} = t_\mathrm{c}$ is the coupling parameter between PT molecule and FM electrodes.

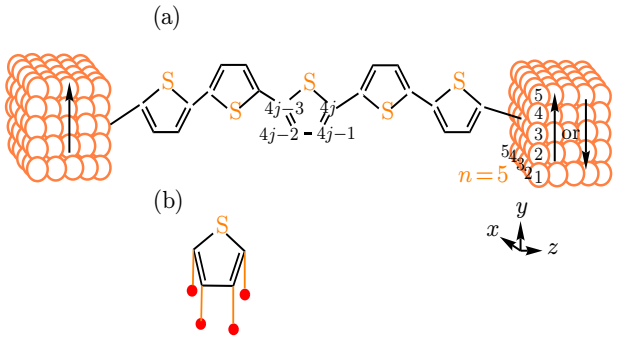


Fig. 1. (color online) (a) The FM/polythiophene/FM junction in both parallel and antiparallel configurations. Here, n refers to the number of thiophene rings and $4j,\ldots,4j-3$ denote to the site of carbon atoms in molecular chain. (b) Each carbon site of PT molecule is assumed to be coupled to a fictitious electronic reservoir to include the dephasing process.

Other parameters in Eq. 6 can be described as: $\Sigma_{\alpha,\sigma}(\varepsilon)$ is the spin-dependent self-energy function that describes the effect of semi-infinite FM electrodes on the molecular chain and is defined as: $\Sigma_{L,\sigma} = \tau^\dagger_{c,L} g_{L,\sigma} \tau_{c,L}$ and $\Sigma_{R,\sigma} = \tau_{R,c} g_{R,\sigma} \tau^\dagger_{R,c}$ where, $g_{L,\sigma}$ and $g_{R,\sigma}$ are surface Green functions for the left and right FM electrodes, respectively, which are calculated in Refs. [34] and [35] as follows:

$$g_{\alpha,\sigma}(i,j;z) = \sum_k \frac{\psi_k(r_i)\psi^*_k(r_j)\sin^2(k_z a)}{z - \varepsilon_0 + \sigma.J_\alpha + \varepsilon(k)}, \tag{14}$$

where, $r_i \equiv (x_i, y_i, z_i)$, $\boldsymbol{K} \equiv (l_x, l_y, k_z)$, $z = \varepsilon_0 + \mathrm{i}0^+$,

$$\psi_k(r_i) = \frac{2\sqrt{2}}{(N_x+1)(N_y+1)N_z} \times \sin\left(\frac{l_x x_i \pi}{N_x+1}\right) \sin\left(\frac{l_y y_i \pi}{N_y+1}\right) \sin(k_z z_i), \tag{15}$$

and

$$\varepsilon(\boldsymbol{k}) = 2t\left[\cos\left(\frac{l_x\pi}{N_x+1}\right) + \cos\left(\frac{l_y\pi}{N_y+1}\right) + \cos(k_z a)\right], \tag{16}$$

Here, $l_{x,y}(=l,\ldots,N_{x,y})$ are integers, $k_z \in [-\pi/a, \pi/a]$, and N_β $(\beta = x,y,z)$ is the number of lattice sites in β direction. N_x and N_y denote the number of atoms at the cross section of the FM electrodes, ε_0 is the on-site energy in the electrodes and will be set to t and t is the hopping strength between the nearest neighbor sites in the electrodes. $\tau_{\alpha,c}$ is the coupling matrix and is non-zero only for the near neighbor points in the molecule and the electrode α. Following the Büttiker probe method, the effect of dephasing is modeled phenomenologically by coupling each carbon site to one fictitious electron reservoir, as indicated in Fig. 1(b). We assume that the net current flowing through these probes is zero, so the electron transport remains elastic although incoherent and currents (Eqs. (1a)–(1c)) could be expressed by the formula similar to the Landauer formula.[36] Therefore, the fictitious probes can be affected in our system through a scattering self-energy term, as follows:[37]

$$\Sigma_D = \sum_{k=1}^{N} -\mathrm{i}\gamma_k c^\dagger_k c_k. \tag{17}$$

Here, N refers to the number of carbon atoms in the molecular chain. The coupling terms $\Gamma_{L,\sigma}$ and $\Gamma_{R,\sigma}$ can be calculated through the expression[38]

$$\Gamma_{\alpha,\sigma} = \mathrm{i}[\Sigma^r_{\alpha,\sigma} - \Sigma^a_{\alpha,\sigma}], \tag{18}$$

where, advanced self-energy $\Sigma^a_{\alpha,\sigma}$ is the Hermitian conjugated of the retarded one.

In order to compute the charge and spin thermoelectric properties of the PT molecular junction in the linear response regime, the charge, heat and spin currents are expanded by temperature gradient, ΔT, and induced voltage drop, ΔV, to first order as follows:

$$J_\mathrm{e} = e^2 \sum_\sigma L_{0\sigma} \Delta V + \frac{e}{T} \sum_\sigma L_{1\sigma} \Delta T, \tag{19a}$$

$$J_\mathrm{Q} = e \sum_\sigma L_{1\sigma} \Delta V + \frac{1}{T} \sum_\sigma L_{2\sigma} \Delta T, \tag{19b}$$

$$J_\mathrm{s} = e \sum_\sigma L_{0\sigma} \frac{\hbar}{2} \sigma \Delta V + \frac{1}{T} \sum_\sigma L_{1\sigma} \frac{\hbar}{2} \sigma \Delta T, \tag{19c}$$

where

$$L_{n\sigma} = -\frac{1}{h} \int \mathrm{d}\varepsilon (\varepsilon - \mu_L)^n \frac{\partial f}{\partial \varepsilon} T_{\mathrm{eff}\sigma}(\varepsilon). \tag{20}$$

The charge and spin thermoelectric coefficients are given as follows:[39,40] the ratio of the induced voltage drop to applied temperature gradient is charge thermopower, S, when the $J = 0$. Also, spin thermopower, S_s is the ratio of the induced spin voltage drop to the applied temperature gradient when the charge and spin currents vanish ($J = 0$ and $J_\mathrm{s} = 0$), therefore,

$$S = -\frac{1}{2eT}\left(\frac{L_{1\uparrow}}{L_{0\uparrow}} + \frac{L_{1\downarrow}}{L_{0\downarrow}}\right),$$

and

$$S_\mathrm{s} = -\frac{1}{2eT}\left(\frac{L_{1\uparrow}}{L_{0\uparrow}} - \frac{L_{1\downarrow}}{L_{0\downarrow}}\right)$$

are charge and spin thermopowers, respectively. The spin dependent thermopower is given as

$$S_\sigma = -\frac{1}{eT}\left(\frac{L_{1\sigma}}{L_{0\sigma}}\right).$$

The spin and charge conductances (G_s and G_e, respectively) are given by:

$$G_s = e\sum_\sigma \left(L_{0\sigma}\frac{\hbar}{2}\sigma\right), \tag{21a}$$

$$G_e = e^2\sum_\sigma L_{0\sigma}. \tag{21b}$$

Finally, the thermal conductance, κ, is as follows:

$$\kappa = \frac{1}{T}\sum_\sigma \left[L_{2\sigma} - \frac{L_{1\sigma}^2}{L_{0\sigma}}\right]. \tag{22}$$

3. Results and discussion

In this section, we describe the numerical results for disordered PT chain connected to FM electrodes. The direction of magnetization in the left FM electrode is fixed in the $+y$ direction while the magnetization in the right electrode is free to flip into either the $+y$ direction, parallel (P) configuration or $-y$ direction, antiparallel (AP) configuration, see Fig. 1(a). We set $|J_\alpha| = 1.5$ eV, $t = 1$ eV, $\varepsilon_0 = 1$ eV for the FM electrodes.[37] For PT molecular chain, we have $K_0 = 21$ eV/Å^2, $\varepsilon_j = -4.3$ eV, $t_0 = 2.5$ eV, $t_1 = 0.675$ eV, $\varepsilon_s = t_s = 0.05t_0$, $\alpha = 4.3$ eV/Å.[32] Also, we regard $T = 11$ K, $t_c = 0.5$ eV, $\gamma = 0.005$ eV, and $E_f = 0$. In this study, the temperature is low enough to consider the no spin-flip process.

Figure 2 shows the dependence of the charge thermoelectric properties on the gate voltage for the PT molecule with five rings in presence and absence of the fictitious probes in parallel configuration. It is obvious from Fig. 2(a) that by increasing γ, G_e decreases. It can be found from the effective transmission coefficient of the junction. One can see from the inset of Fig. 2(a) that the height of $T_{\text{eff}}(\varepsilon)$ peak decreases in the presence of dephasing due to increase of resistance to charge transport because of the enhanced probability to backscatter the charge via fictitious probes.[2] It is also observed from the inset of Fig. 2(a) that the peak of transmission probability becomes wider in the presence of additional probes ($\gamma \neq 0$) in comparison with $\gamma = 0$. This broadening arises from the dominance of the randomizing effect over backscattering as a consequence of phase incoherency in the dephasing process.[29] Because of the better clarity, we indicate only one of the $T_{\text{eff}}(\varepsilon)$ peaks in the inset of Fig. 2(a). The peak becomes wider and its height decreases by increasing γ due to more scattering rate.

The charge thermopower and figure of merit are indicated in Figs. 2(b) and 2(c). The thermopower of PT has an oscillating behavior, denoting the change in the number of electrons in the molecular energy levels[41–43] and decreases in the presence of dephasing. The value of S decreases more by γ because of of the larger scattering in atomic sites of the molecular chain. In the strong coupling regime, the number of oscillation of the peaks decreases because the $T_{\text{eff}}(\varepsilon)$ peaks almost disappear in the greater value of γ. The main factor for the shape of ZT is charge thermopower. The ZT is zero in points that $S = 0$ and the extremum points of S are the extremums of ZT. Therefore, the value of the ZT decreases by increasing γ.

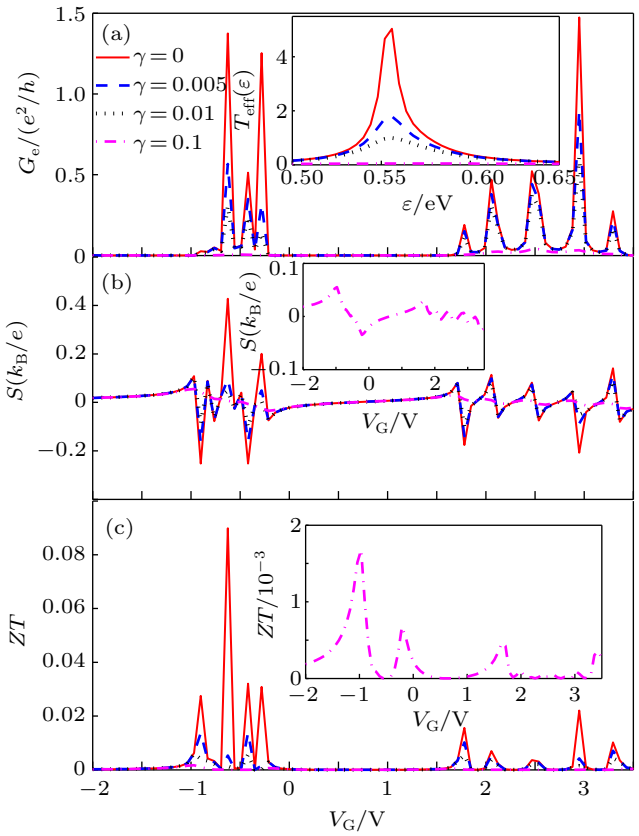


Fig. 2. (color online) The charge thermoelectric properties of PT ($n = 5$) for different γ: (a) electrical conductance, (b) charge thermopower, (c) charge figure of merit. The insets show (a) the effective transmission coefficient for different γ, (b) charge thermopower in $\gamma = 0.1$ eV, (c) charge figure of merit in $\gamma = 0.1$ eV. $T = 11$ K and $E_f = 0$.

The electrical and spin conductances in the presence of the additional probes for three consecutive lengths of PT chain ($n = 5, 6$, and 7) are indicated in Fig. 3 versus gate voltage in both P and AP configurations. The conductance peaks are located in the molecular energy levels and their height decreases by increasing molecular length. It can be found from the change in the effective transmission coefficient. The HOMO–LUMO gap slightly decreases by the chain length enhancement. This comes from the change in the arrangement of the π-electron levels of the molecule by increasing the molecular length due to electron-donating characteristic of sulfur atoms in thiophene rings.[44,45] Figures 3(a) and 3(b) show the electrical conductance in P and AP configurations of the electrodes, respectively. The value of G_e in P configuration is more than the AP one because the electrical conductance in P

configuration is controlled by participating tunneling between majority and minority carriers in both FM electrodes. Meanwhile, in the AP alignment the magnetic moments of leads are in the opposite direction and the carriers have to tunnel between the spin-majority and spin-minority bands through the molecular levels; consequently, the charge transport is suppressed. Therefore, the values of both electrical and spin conductances decrease in AP alignment. The spin conductance is the difference between spin-up conductance, $G_{\uparrow}$, and spin-down conductance, $G_{\downarrow}$. In the P configuration, $G_{\rm s}$ has a positive value for all considered lengths (Fig. 3(c), indicating that the spin-up conductance is bigger than spin-down one. But in the AP configuration, the $G_{\rm s}$ value is positive in some gate voltages and in some gate voltages is negative, denoting that in the negative case $G_{\downarrow}$ has bigger value than $G_{\uparrow}$ (See the inset of Fig. 3). It is interesting that the value of $G_{\rm s}$ in AP alignment is much less than in the P alignment because of the larger suppression in the charge transport between electrodes.

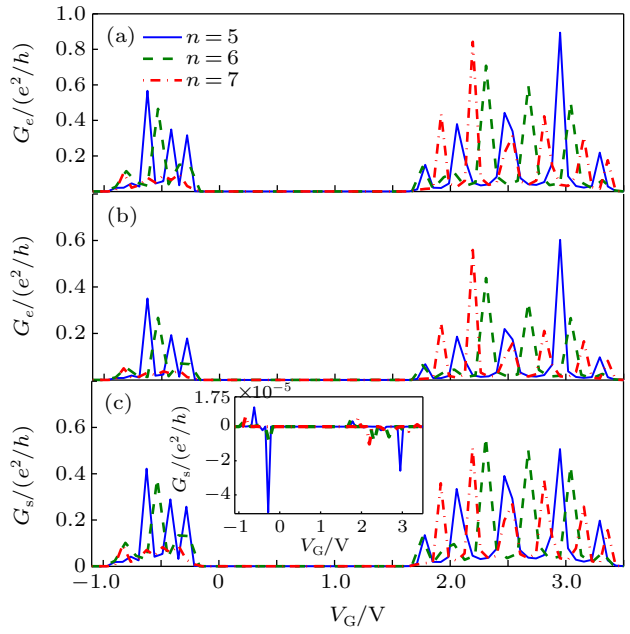


Fig. 3. (color online) Electrical conductance in (a) P and (b) AP configurations, (c) spin conductance in P configuration, versus gate voltage. The inset of panel (c) shows $G_{\rm s}$ in antiparallel alignment. $T = 11$ K and $E_{\rm f} = 0$.

The charge and spin thermopowers as a function of the gate voltage are indicated in Figs. 4(a) and 4(b) for considered lengths of the disordered PT chain. Figure 4(a) and its inset show the charge thermopower in P and AP configurations, respectively. The value and the number of oscillations increase by molecular length enhancement in both configurations.[22,46] It can be found from the increasing number of π-electrons in the PT chain that increasing the molecular length causes the number of electrons tunneling through the molecular level to increase. The thermopower (charge and spin) is zero in resonance energies and electron–hole symmetry points. In the symmetry points, both carriers participating in transport mechanism, have equal contributions but with opposite signs, so the net induced voltage drop is zero and, as a consequence, thermopower becomes zero. In resonance energies, the temperature gradient cannot produce a net electrical current because the electrons can tunnel from the hotter and colder electrodes to the molecular levels without needing thermal energy. The spin thermopower in both P and AP configurations is represented in Fig. 4(b) and its inset, respectively. $S_{\rm s}$ is employed to study the spin effects in the thermoelectric transport, and is the difference between spin-up and spin-down thermopowers, $S_{\uparrow} - S_{\downarrow}$. Similar to charge thermopower, the spin thermopower changes the sign and magnitude with molecular length alternatively when the Fermi level crosses the resonance energy or symmetry points.[10] The positive sign of $S_{\rm s}$ indicates that the $S_{\uparrow}$ is greater than the $S_{\downarrow}$. In fact, the induced spin-up voltage drop is bigger than spin-down one and the negative sign of spin thermopower denotes $S_{\downarrow} > S_{\uparrow}$, whereas the sign of charge thermopower determines the kind of carriers participating in energy and charge transports. It is obvious from the Figs. 4(a) and 4(b) that the sign of charge thermopower is the opposite of the spin thermopower due to the increase of the minority spin voltage.[42,47] Also, the values of both S and $S_{\rm s}$ are decreased in AP configuration with respect to the P configuration due to tunneling between spin-majority and spin-minority carriers and the suppressed transport. The reduction is more obvious in the case of $S_{\rm s}$.

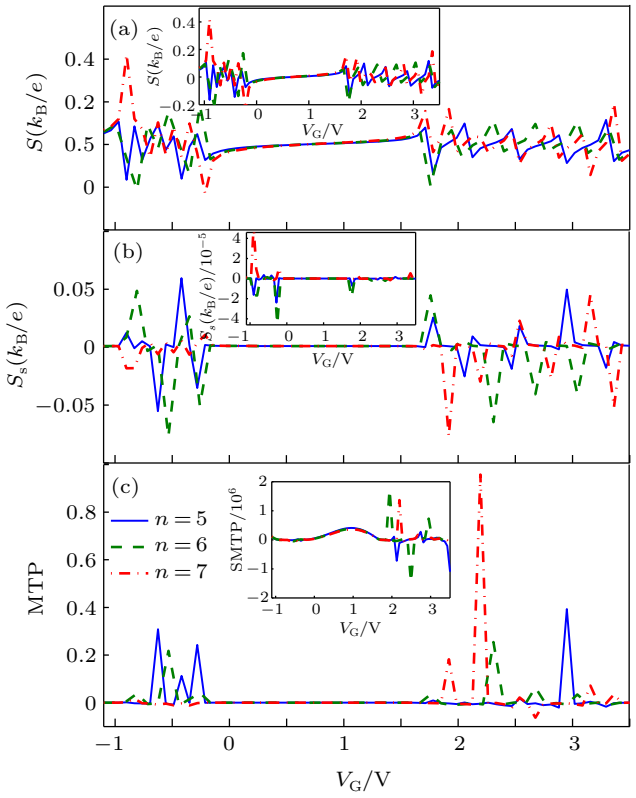


Fig. 4. (color online) (a) Charge thermopower in P configuration versus gate voltage. The inset shows the charge thermopower in the AP configuration. (b) Spin thermopower as a function of gate voltage in P configuration, the inset shows the $S_{\rm s}$ in AP one. (c) The charge magnetothermopower and inset shows the spin magnetothermopower versus gate voltage. $T = 11$ K and $E_{\rm f} = 0$.

The charge thermal tunneling effect from FM electrodes to the molecular levels due to the temperature gradient results in charge magnetothermopower (MTP). On the other hand, the spin thermal tunneling due to spin voltage drop results in spin magnetothermopower (SMTP). These quantities are related to the dependence of the charge and spin thermoelectric effects on the magnetic orientation of the electrodes and are defined as:[48] MTP $= (S(\mathrm{P}) - S(\mathrm{AP}))/(S(\mathrm{AP}))$ and SMTP $= (S_\mathrm{s}(\mathrm{P}) - S_\mathrm{s}(\mathrm{AP}))/(S_\mathrm{s}(\mathrm{AP}))$. The MTP of the different lengths of the PT chain is indicated in Fig. 4(c) versus gate voltage. It is observed from this figure that, the thermal tunneling between carrier bands for $n = 7$ is larger than other lengths in $V_\mathrm{G} = 2.2$ V but in negative gate voltages the MTP (tunneling) is nearly zero. In the case of PT with five rings, the tunneling effect is intensive in $V_\mathrm{G} = -1$ V to $V_\mathrm{G} = 0$, and $V_\mathrm{G} = 3$ V. Also, the thermal tunneling effect can be observed in almost all the molecular energy levels. The gate voltage dependence of SMTP for the considered lengths is shown in the inset of Fig. 4(c). The spin thermal tunneling effect is more significant in the case of $n = 6$ with respect to other lengths. The value of the SMTP is greater than MTP due to existence of big difference between spin thermopowers in parallel and antiparallel configurations.

The figure of merit of the considered lengths of the molecule for P and AP alignments is indicated in Figs. 5(a) and 5(b) versus gate voltage. The number and magnitude of the ZT peaks increase by increasing the molecular length because the same behavior was observed for S in the same configuration. The dependence of the spin figure of merit on the gate voltage for P configuration is plotted in Fig. 5(c). The peaks of $Z_\mathrm{s}T$ are in the points that S_s has extremum and the valleys of it are placed at points that $S_\mathrm{s} = 0$. The value of $Z_\mathrm{s}T$ in AP configuration is considerably less than P one and is near to zero.

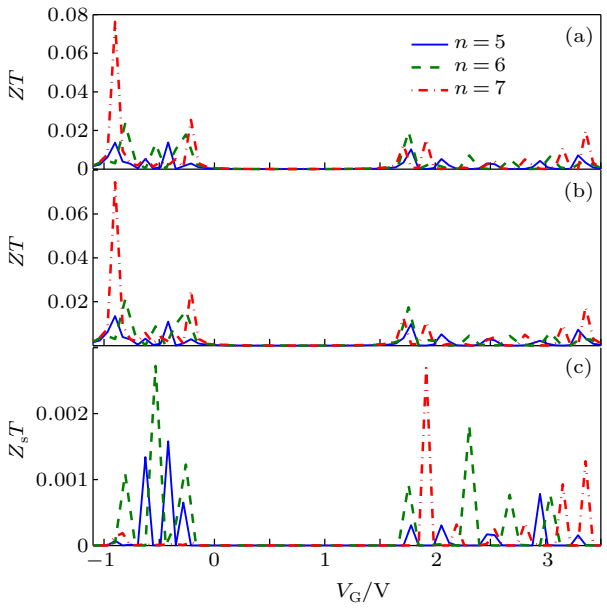


Fig. 5. (color online) Charge figure of merit in (a) parallel and (b) antiparallel configurations. (c) Spin figure of merit for P configuration versus gate voltage. $T = 11$ K and $E_\mathrm{f} = 0$.

The temperature dependence of the charge thermoelectric properties for the different disordered molecular lengths are shown for P configurations in Fig. 6. The electrical conductance increases by the length due to decreasing the HOMO–LUMO gap and the distance of energy levels (see Fig. 6(a). It

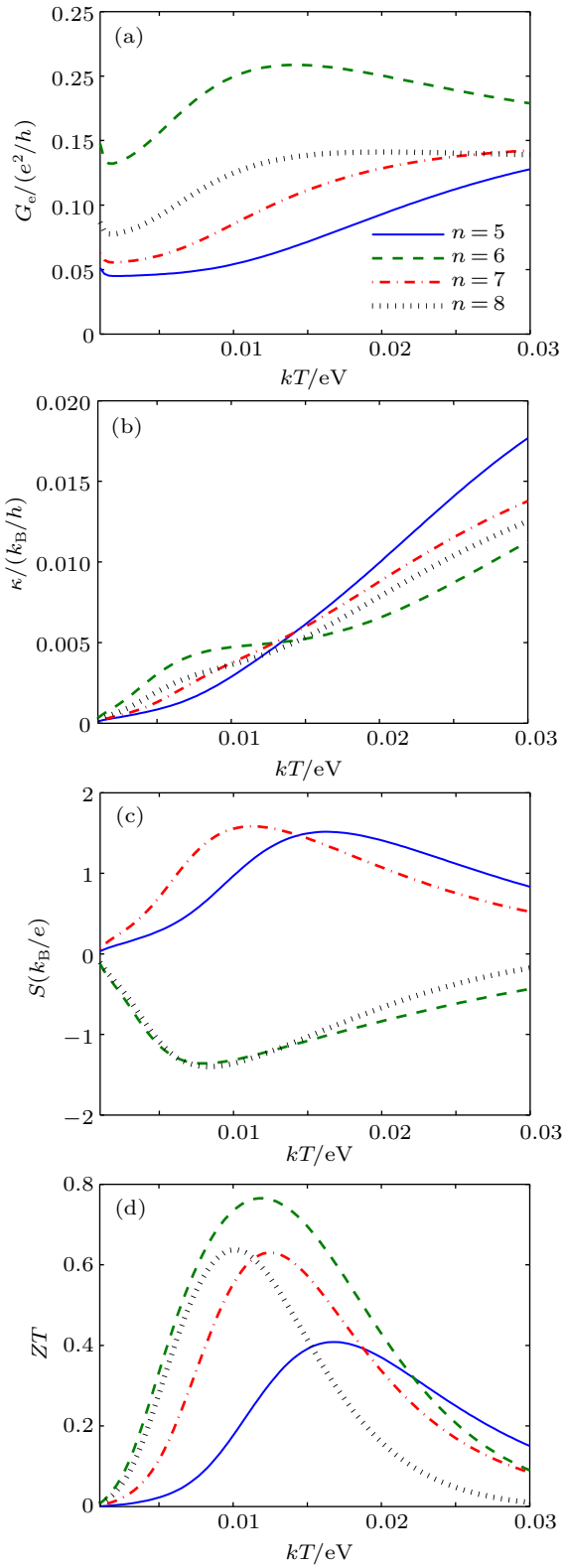


Fig. 6. (color online) Charge thermoelectric coefficients versus temperature for different lengths of disordered polythiophene chain in P alignment: (a) electrical conductance, (b) thermal conductance, (c) charge thermopower, and (d) charge figure of merit. We set $V_\mathrm{G} = 0$ and $E_\mathrm{f} = 0$.

causes the number of tunneling electrons to increase. The electrical conductance increases by the temperature in each length of the molecular chain. The effective transmission coefficient is independent of the temperature but the Fermi derivative is temperature dependent. By increasing the temperature, $(-\partial f/\partial\varepsilon)$ is broadened and more parts of $T_{\rm eff}(\varepsilon)$ can be covered by $(-\partial f/\partial\varepsilon)$, so the number of electrons participating in transport increases. The magnitude of $G_{\rm e}$ for PT molecule with six thiophene rings is bigger than other considered PT lengths. It can be found from the Figs. 7(a)–7(c) that the $T_{\rm eff}(\varepsilon)$ peaks are more included in $(-\partial f/\partial\varepsilon)$ for $n=6$ with respect to the other lengths ($n=5$ and $n=7$). Therefore, the number of tunneling carriers increases and $G_{\rm e}$ becomes bigger than the others.

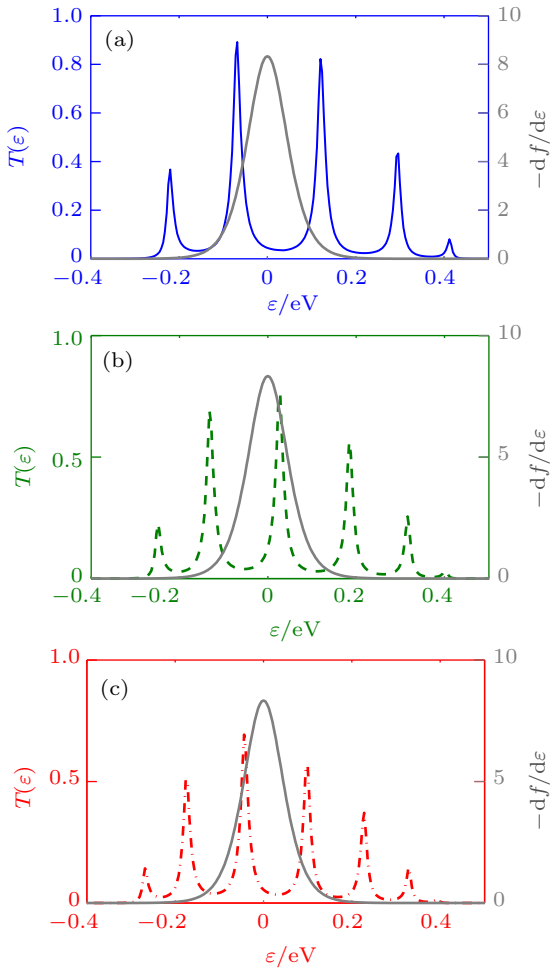


Fig. 7. (color online) Transmission coefficient peaks in (a) $n=5$, (b) $n=6$, and (c) $n=7$. The Fermi derivative is indicated in gray.

The thermal conductance versus temperature is shown Fig. 6(b) for different lengths of the PT molecular chain. It is obvious that the $n=5$ has maximum value for κ with respect to other lengths. Figure 6(c) indicates the charge thermopower as a function of temperature. As mentioned in the description of Fig. 4, the sign of charge thermopower shows the kind of carrier participating in the transport mechanism. For the molecular chain with even number of thiophene rings, S is negative, indicating that the electrons are responsible for energy and charge transports in the chain, also, the Fermi level is located near to LUMO level. Whereas, the sign of S for odd number of thiophene rings shows that the holes are dominant for the transport mechanism in the junction and the Fermi level is located near to HOMO level.

The temperature dependence of the charge figure of merit for the considered lengths of disordered chain is shown in Fig. 6(d). The ZT reaches to a maximum and then decreases by the temperature enhancement. This can be found from the curve of S. The maximum value of the ZT almost increases by increase of the thiophene rings. In the case of $n=6$, ZT has maximum value in comparison with other consecutive lengths, because the $G_{\rm e}$ is maximum and κ is minimum for $n=6$. The same behaviors are observed in AP configuration but the value of the coefficients is decreased due to the suppression of transport in this alignment.

4. Summary

In this work, we have studied the charge and spin thermoelectric properties of polythiophene molecular junction with ferromagnetic electrodes in both parallel and antiparallel configurations. We have introduced the dephasing process with a phenomenological Büttiker probe model. Our method is based on a tight-binding model within Green function formalism that can help to find the charge and spin thermoelectric coefficients of a disordered PT chain in the linear response regime. Our results show the decrease of thermoelectric coefficients in both configurations is due to the decrease of height and increase of wide of effective transmission coefficient peaks. By increasing incoherency, the decrease is more obvious. We have also found that the SMTP versus energy levels is greater than MTP (charge thermal tunneling) due to big difference between spin thermopowers in parallel and antiparallel alignments respect to charge thermopower. In addition, the sign of thermopower is affected by the number of thiophene rings in the chain. Therefore, the kind of carrier controlling transport also changes.

References

[1] Zhag Y, Zelinskyy Y and May V 2013 *Phys. Rev. B* **88** 155426
[2] Wierzbinski E, Venkatramani R, Davis K L, Bezer S, J. Kong, Xing Y, Borguet E, Achim C, Beratan D N and Waldeck D H 2013 *ACS Nano* **7** 5391
[3] Nozaki D, Gomes da Rocha C, Pastawski H M and Cuniberti G 2012 *Phys. Rev. B* **85** 155327
[4] Lai W, Xing Y and Ma Z 2013 *J. Phys.: Condens. Matter* **25** 205304
[5] Lai W, Zhang Ch and Ma Z 2015 *Front. Phys.* **10** 59
[6] Büttiker M 1986 *Phys. Rev. Lett.* **57** 1761
[7] DAmato J L and Pastawski H M 1990 *Phys. Rev. B* **41** 7411
[8] Rejec T, Žitko R, Mravlje J and Ramšak A 2012 *Phys. Rev. B* **85** 085117
[9] Andergassen S, Costi T A and Zlatić V 2011 *Phys. Rev. B* **84** 241107
[10] Zheng J, Chi F and Guo Y 2012 *J. Phys.: Condens. Matter* **24** 265301
[11] Bergfield J P, Solis M and Stafford C A 2010 *ACS Nano* **4** 5314
[12] Wei J H, Liu X. J, Xie S J and Yan Y 2009 *J. Chem. Phys.* **131** 064906
[13] Yakuphanoglu F, Liu H T and Xu J K 2007 *J. Phys. Chem. B* **111** 7535
[14] Hiroshigo Y, Ookawa M and Toshima N 2007 *Synthetic Metals* **157** 647
[15] Malen J A, Doak P, Baheti K, Tilley T D, Segalman R A and Majumdar A 2009 *Nano Lett.* **9** 1164
[16] Bubnova O, Berggren M and Crispin X 2012 *J. Am. Chem. Soc.* **134** 16456
[17] Rittmeyer S P and Groß A 2012 *Beilstein J. Nanotechnol.* **3** 909

[18] Gao X, Uehara K, Klug D D, Patchkovskii S, Tse J S and Tritt T M 2005 *Phys. Rev. B* **72** 125202
[19] Fu J Y, Liu D S and Xie S J 2008 *Physica E* **40** 915
[20] Lu B Y, Liu C C, Lu S, Xu J K, Jiang F K, Li Y Zh and Zhang Z 2010 *Chin. Phys. Lett.* **27** 057201
[21] Wei J H, Liu X J, Xie S J and Yan Y 2009 *J. Chem. Phys.* **131** 064906
[22] Pauly F, Viljas J K and Cuevas J C 2008 *Phys. Rev. B* **78** 035315
[23] Popescue A and Haney P M 2012 *Phys. Rev. B* **86** 155452
[24] Golizade-mojarrad R and Datta S 2007 *Phys. Rev. B* **75** 081301
[25] Dutta P, Maiti S K and Karmakar S N 2010 *Organic Electronics* **11** 1120
[26] Su W P, Schrieffer J R an Heeger A 1980 *Phys. Rev. B* **22** 2099
[27] Datta S 2005 *Quantum Transport: Atom to Transistor* (Camberige: Cambridge University Press)
[28] Meir Y and Wingreen N S 1992 *Phys. Rev. Lett.* **68** 2512
[29] Dey M, Maiti S K and Karmakar S N 2011 *Organic Electronics* **12** 1017
[30] Kang Y M, Xie Z, An Zh, Li Y Ch and Chen N X 2003 *J. Phys. Chem. Solids* **64** 377
[31] Wei J H, Xie S J, Mei L M, Berakdar J and Yan Y 2007 *Organic Electronics* **8** 487
[32] Hu G C, Wei J H and Xie S J 2007 *Appl. Phys. Lett.* **91** 142115
[33] Xie S J, Mie L M and Lin D L 1994 *Phys. Rev. B* **50** 13364
[34] Yoshihiro A and F. Hidetoshi 2005 *Phys. Rev. B* **72** 085431
[35] Yaghobi M and Yuonesi M 2012 *Mol. Phys.* **110** 49
[36] Zimbovskaya N A 2013 *Transport Properties of Molecular Junctions* (Berlin: Springer Tracts in Modern Physics, Springer)
[37] Ahmadi Fouladi A, Ketabi S A, Elahi S M and Sebt S A 2012 *Eur. Phys. J. B* **85** 163
[38] Datta S 1997 *Electronic transport in mesoscopic systems* (Cambridge: Cambridge University Press)
[39] Trocha P and Barnas J 2012 *Phys. Rev. B* **85** 085408
[40] Liu Y S, Chi F, Yang X F and Feng J F 2011 *J. Appl. Phys.* **109** 053712
[41] Bagheri Tagani M and Rahimpour Soleimani H 2012 *J. Appl. Phys.* **112** 103719
[42] Bagheri Tagani M and Rahimpour Soleimani H 2013 *J. Appl. Phys.* **113** 143709
[43] Bagheri Tagani M and Rahimpour Soleimani H 2012 *Solid State Commun.* **152** 914
[44] Golsanamlou Z, Izadi Vishkayi S, Bagheri Tagani M and H. Rahimpour Soleimani 2014 *Chem. Phys. Lett.* **594** 51
[45] Zeng C, Li B, Wang, Wang H, Wang K, Yang J, Hou J G and Zhu Q 2002 *J. Chem. Phys.* **117** 851
[46] Viljas J K, Pauly F and Cuevas J C 2008 *Phys. Rev. B* **77** 155119
[47] Świrkowicz R, Wierzbicki M and Barnaś J 2009 *Phys. Rev. B* **80** 195409
[48] Golsanamlou Z, Bagheri Tagani M and Rahimpour Soleimani H 2014 *Macromolecular Theory and Simulations* **23** 311